PHYSICAL REVIEW A **78**, 010101(R) (2008)

Mesoscopic spin-boson models of trapped ions

D. Porras,[1] F. Marquardt,[2] J. von Delft,[2] and J. I. Cirac[1]
[1]*Max-Planck Institut für Quantenoptik, Hans-Kopfermann-Strasse 1, Garching D-85748, Germany*
[2]*Physics Department, Arnold Sommerfeld Center for Theoretical Physics, and Center for NanoScience, Ludwig-Maximilians-Universität München, 80333 München, Germany*
(Received 29 October 2007; revised manuscript received 29 February 2008; published 2 July 2008)

Trapped ions arranged in Coulomb crystals provide us with the elements to study the physics of a single spin coupled to a boson bath. In this work, we show that optical forces allow us to realize a variety of spin-boson models, depending on the crystal geometry and the laser configuration. We study in detail the ohmic case, which can be implemented by illuminating a single ion with a traveling wave. The mesoscopic character of the phonon bath in trapped ions induces effects such as the appearance of quantum revivals in the spin evolution.

DOI: 10.1103/PhysRevA.78.010101 PACS number(s): 03.65.Yz, 05.30.Jp, 37.10.Vz

The problem posed by a two-level system interacting with a bath of harmonic oscillators, known as the spin-boson model, appears in condensed matter, atomic physics, and quantum-information processing. It is of fundamental importance, since it represents a paradigm for the study of quantum dissipation and the quantum-to-classical transition [1,2]. The spin-boson model displays nonperturbative features, such as the inhibition of spin relaxation above a critical dissipation strength, known as the localization transition. Despite its fundamental importance, experimental investigations into anything but the weak-coupling regime of the spin-boson model are still scarce. The localization transition has been observed in the related Josephson junction systems [3], while typical solid-state two-level systems feature a coupling strength much below the critical threshold [4].

Trapped ions provide a clean system ideally suited for the quantum simulation of condensed-matter problems [5,6]. In this Rapid Communication, we show that they also offer realizations, with a wide range of tunable parameters, of the spin-boson model (σ_x, σ_z are Pauli matrices, $\hbar \equiv 1$),

$$H = \frac{\epsilon}{2}\sigma_z + \frac{\Delta}{2}\sigma_x + H_B + \frac{\sigma_z}{2}\sum_n (\lambda_n a_n^\dagger + \lambda_n^* a_n). \qquad (1)$$

We consider a Coulomb crystal of identical ions, each having two hyperfine levels split by internal energy ω_0. Their vibrational normal modes constitute a phonon bath, $H_B = \Sigma_n \omega_n (a_n^\dagger a_n + \frac{1}{2})$, whose eigenfrequencies ω_n depend on both the vibrational directions and trapping conditions. By focusing one or more laser beams onto a single ion in the crystal, henceforth called the "central ion," several types of couplings between its two hyperfine levels, say $|\pm 1\rangle$ (taken to be eigenstates of σ_z), and the phonon modes can be induced [7], leading to several types of realizations of the spin-boson model (see Fig. 1). This offers a wide range of possibilities for observing the phenomenology of the spin-boson model, with the advantage that well-developed experimental techniques exist for the preparation of both the initial spin and phonon bath states [8]. Moreover, the vibrational modes, being finite in number, form a *mesoscopic* (not macroscopic) environment. This leads to interesting memory effects such as quantum revivals in the spin evolution, which are absent in the customary limit of a macroscopic bath.

Our main results are as follows. (i) One-dimensional (1D) and 2D Coulomb crystals yield a variety of power-law phonon spectral densities, $J(\omega) \propto \omega^s$, ranging from sub ohmic ($s<1$) to super ohmic ($s>1$), depending on the ion crystal dimension and the laser configuration. (ii) In particular, by addressing the central ion by a traveling wave laser field, the ohmic ($s=1$) spin-boson model can be realized with tunable interaction strength, allowing the standard phenomenology of this model, such as the localization transition, to be realized if the number of ions is large enough. (iii) For time scales larger than a given revival time, finite-size effects induce the re-excitation of the spin after an initial period of relaxation (quantum revival), which can be observed in a wide range of parameters, including high phonon temperatures.

REALIZATIONS OF SPIN-BOSON COUPLING

Let the central ion's coordinate relative to its equilibrium position, in the direction of the optical force (specified below), be represented by the operator $z = \Sigma_n \mathcal{M}_n \bar{z}_n (a_n + a_n^\dagger)$. Here $\bar{z}_n = 1/\sqrt{2m\omega_n}$, m is the ion mass, and $\mathcal{M}_n$ is the amplitude of vibrational mode n at the central ion, which is readily calculated by finding the normal modes of the Coulomb chain in the harmonic approximation; see [5]. We now consider two different setups, in which the tunneling and spin-boson coupling terms of Eq. (1) are generated (i) by two separate laser fields or (ii) by a single laser field, respectively.

(i) State-dependent dipole force from a standing wave. This setup requires two laser fields. The first couples to the central ion's internal states in such a way that its frequency

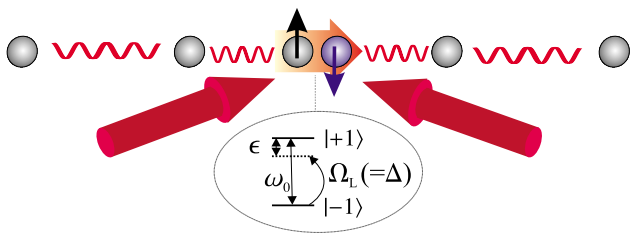

FIG. 1. (Color online) Scheme for the implementation of spin-boson couplings in Coulomb chains.

ω_L and Rabi frequency Ω_L set the bias $\epsilon=\omega_0-\omega_L$ and tunneling amplitude $\Delta=\Omega_L$. The second laser field is an off-resonant standing wave with wave number k and phase ϕ, which creates a state-dependent dipole potential $V(z)=V_0\cos^2(kz+\phi)\sigma_z$, thus inducing a spin-boson coupling. In the Lamb-Dicke regime ($kz\ll 1$) we can expand $V(z)$ to obtain

$$H_{\rm sw}=V_0[\cos^2\phi-kz\,\sin 2\phi-(kz)^2\cos 2\phi]\sigma_z. \qquad (2)$$

The first term just shifts the bias ϵ, and one can choose to eliminate the second or third term by setting $\phi=0$ or $\pi/4$, respectively. The latter choice yields Eq. (1), with $\lambda_n^{\rm sw}=-2kV_0\mathcal{M}_n\bar{z}_n$ and $\epsilon=\omega_0-\omega_L+V_0$.

(ii) Polaron coupling from a traveling wave. In this setup, a single laser field produces a traveling wave focused on the central ion, such that the coupling is given, in a frame rotating with ω_L, by

$$H_{\rm tw}=\frac{\Omega_L}{2}(\sigma^+e^{ikz}+\sigma^-e^{-ikz}). \qquad (3)$$

This system is unitarily related to that of Eq. (1), and hence shows the same quantum dynamics. Indeed, using the canonical transformation $U=e^{-(i/2)kz\sigma^z}$, the Hamiltonian $U[H_B+H_{\rm tw}+(\omega_0-\omega_L)\sigma^z]U^\dagger$ readily reduces to Eq. (1), with $\lambda_n^{\rm tw}=-ik\bar{z}_n\mathcal{M}_n\omega_n$, $\Delta=\Omega_L$, and $\epsilon=\omega_0-\omega_L$.

SPECTRAL DENSITY

The properties of the spin-boson model are determined by the spectral density, $J(\omega)=\pi\Sigma_{n=1}^N|\lambda_n|^2\delta(\omega-\omega_n)$. A finite number N of phonon modes have a discrete spectrum leading to finite-size effects, to be discussed below. However, to gain qualitative understanding, we first consider the thermodynamic limit ($N\to\infty$) of a continuous spectrum. We focus on experimental conditions leading to an approximately gapless bath, namely, 1D and 2D Coulomb crystals: their axial (1D) or in-plane (2D) modes are approximately gapless, since their minimum energy, say ω_z, is the global trapping frequency (corresponding to the center-of-mass frequency), which has to be sufficiently small to guarantee the stability of the crystal. For a 1D Coulomb chain of N ions, the energy spectrum of axial vibrations with $1\ll n\ll N$ is $\omega_n^{\rm 1D}=\overline{\delta\omega}n[1+\frac{2}{3}\log(\frac{N}{\pi n})]^{1/2}$ [9], where $\overline{\delta\omega}=r\omega_z$, $r=(\pi/N)\sqrt{3e^2/(m\omega_z^2d_0^3)}$, and d_0 is the distance between ions. r is determined by N, such that for mesoscopic Coulomb chains ($N\approx 10^2$) $r\approx 1$ [10]. Qualitative insights can be gained by retaining the factor linear in n only [see Fig. 2(a), solid line], yielding the following spectral densities:

$$J_{\rm sw}^{\rm 1D}(\omega)=\frac{\pi}{Nr}(2V_0k\bar{z})^2\omega^{-1}, \qquad (4)$$

$$J_{\rm tw}^{\rm 1D}(\omega)=\frac{\pi}{Nr}(k\bar{z})^2\omega=2\pi\alpha\omega. \qquad (5)$$

Here we have used that $|\mathcal{M}_n|^2\approx 1/N$, since in the thermodynamic limit vibrational modes are given by plane waves. For $J_{\rm tw}^{\rm 1D}(\omega)$ we introduced the dimensionless dissipation strength

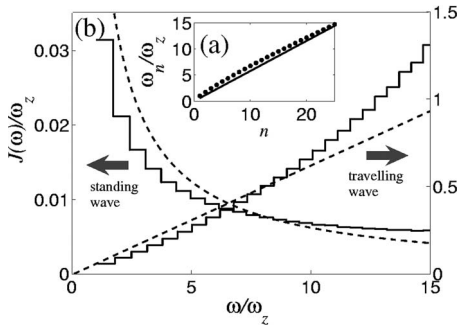

FIG. 2. Phonon bath properties of a Coulomb chain with $N=50$. (a) Dots: Exact axial vibrational spectrum. Continuous line: Approximation $\omega_n^{\rm 1D}\simeq\overline{\delta\omega}n$. (b) Spectral density of spin-boson couplings induced by a standing wave (with $k\bar{z}_1=1$) or a traveling wave (with $2V_0k\bar{z}/\omega_z=1$). The continuous lines are obtained with the exact vibrational spectrum, by substituting the δ function in $J(\omega)$ by a constant function in each interval (ω_n,ω_{n+1}), of height $(\omega_{n+1}-\omega_n)^{-1}$. The dashed lines are the approximations of Eqs. (4) and (5).

α [1]. Finite-size effects will modify the spectral density of a Coulomb crystal. Nevertheless, Eqs. (4) and (5) allow us to determine the character of the phonon bath, as well as the scaling of its properties with experimental parameters. This is shown by the comparison with exact numerical calculations in Fig. 2. Finally, in a 2D Coulomb crystal, ions arrange themselves in a triangular lattice [11]. There, the lowest-energy vibrational modes also show a linear dispersion relation [12], such that the corresponding spin-boson models have an algebraic spectral density with exponents $s=0$ [13] and $s=2$, in the cases of interaction with a standing wave or a traveling wave, respectively.

TRAPPED ION OHMIC MODEL

In the following, we analyze in detail the ohmic case of Eq. (5). Assume that at $t<0$ the coupling is off, the phonon bath is in thermal equilibrium, and the internal state is prepared in $|1\rangle$ by using standard optical pumping techniques. We focus on the evolution of the system at time $t>0$ upon suddenly switching on Eq. (3). In particular, we calculate $P(t)=\langle\sigma^z\rangle$ to determine the evolution of the spin under the effect of the tunneling Δ [1]. The theoretical description of this system can be addressed within the noninteracting blip approximation (NIBA),

$$\dot{P}(t)=\int_0^t K(t-t')P(t')dt',$$

$$K(\tau)=-\Delta^2{\rm Re}\langle e^{ikz(\tau)}e^{-ikz(0)}\rangle, \qquad (6)$$

where the average is evaluated assuming a thermal state in the bosonic bath. This expression can be obtained by neglecting spin-bath correlations in an expansion up to second order in Δ [15]. It is well established [1] that in the case of a continuous ohmic model, the NIBA describes correctly the two limits of weak and strong dissipation, as well as the high-temperature limit.

The finite-size properties of the spin-boson model defined by Eq. (3) can be qualitatively understood by considering the approximation that vibrational energies are equally spaced by a given energy $\delta\omega$ [14]. Then the kernel $K(\tau)$ defined by Eqs. (6) is periodic, and can be written as $K(\tau)=\Sigma_n \bar{K}(\tau-\tau_n)$, $\tau_n=n\tau_{\mathrm{rev}}$, where $\tau_{\mathrm{rev}}=2\pi/\delta\omega$ is the vibrational bath revival time. $\bar{K}(\tau)$ becomes equal to the kernel of the continuum ohmic model in the limit $\delta\omega\to 0$. At short times ($t\ll\tau_{\mathrm{rev}}$), the spin evolution is governed by $\bar{K}(\tau)$, and it behaves similarly to the case of a continuum spin-boson model. The periodic structure of $K(\tau)$ manifests itself at long times ($\tau\geq\tau_{\mathrm{rev}}$) in the form of quantum revivals in $P(t)$. For the 1D trapped ion spin-boson model, the level spacings $\delta\omega_n=(\omega_{n+1}^{\mathrm{1D}}-\omega_n^{\mathrm{1D}})$ deviate from the constant value $\delta\omega$ by logarithmic corrections. However, since these deviations scale like $(\delta\omega_{n+1}-\delta\omega_n)\sim\delta\omega/n$ for large n, the fraction of modes for which they are significant becomes negligible in the limit of large N. Thus, $\tau_{\mathrm{rev}}\approx 2\pi/\delta\omega$ defines the time scale that separates the short-time regime, where $P(t)$ evolves as for a continuous bath, from the long-time regime, displaying quantum revivals.

NUMERICAL SOLUTION

To verify this conclusion, we obtain the numerical solution of $P(t)$ within the NIBA, using the exact vibrational modes of a finite-size ion chain trapped in a harmonic potential. In order to compare these results with those predicted by the ohmic spin-boson model with a continuous bath, we fit the exact low-energy spectral density to the form given by Eq. (5) and thus extract the dissipation strength α. The NIBA can be justified for a discrete phonon bath as long as the decay time of $\bar{K}(\tau)$ is much smaller than τ_{rev}. At short times $t\ll\tau_{\mathrm{rev}}$, the validity of the NIBA in the continuous case implies that the average in Eq. (6) can be calculated by factorizing the total density matrix into spin and phonon reduced density matrices. Due to the periodic structure of $K(\tau)$, brought about by the discreteness of the vibrational bath, we conclude that $P(t)$ is related to the state of the system at times $t-n\tau_{\mathrm{rev}}$. In the first revival ($t\approx\tau_{\mathrm{rev}}$), $P(t)$ depends on the state of the system at short times, where the spin-bath decoupling scheme, which leads to the NIBA, works. Thus, the first revival is well described within the NIBA, and the argument can be easily extended to later revivals. The NIBA integro-differential equation is solved numerically following Ref. [16]. We now discuss in detail the results of the unbiased case ($\epsilon=0$) for two different regimes, having high or low phonon temperatures, respectively.

HIGH-TEMPERATURE REGIME

For sufficiently high temperatures, the kernel $\bar{K}(\tau)$ decays exponentially with a memory time $\tau_m=1/(2\pi\alpha T)$ (we set $k_B=1$). In the continuum limit one finds two main regimes: $\tau_m\Delta>1$ (coherent oscillations), where $P(t)$ oscillates with Δ and decays in a time τ_m; and $\tau_m\Delta<1$ (overdamped relaxation), where $P(t)$ decays with a rate $\Gamma=\Delta^2\tau_m$. In the case of a finite Coulomb chain, $K(\tau)$ shows an exponential decay at short times, and additionally, an approximate periodic structure at time scales $\tau_{\mathrm{rev}}\approx 2\pi/\delta\omega$ [see Fig. 3(b)]. Figure 3(a) shows that the behavior of $P(t)$ at short times clearly reveals the transition between the overdamped and underdamped regimes, as well as the quantum revivals at τ_{rev}. The revival effect can be understood in terms of the perturbation of the Coulomb chain created during the initial spin relaxation, which propagates along the chain, is reflected at the boundaries, and returns to the selected ion, thus inducing its reexcitation. Interesting geometrical effects on the revivals may also be expected in 2D setups. Revivals in the high-temperature regime could be easily observed in experiments with trapped ions, since they require neither cooling to very low temperatures nor high values of α.

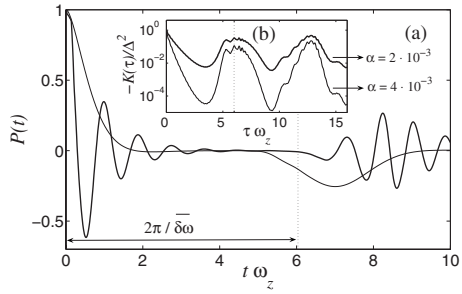

FIG. 3. (a) Transition from the underdamped (thick line, $\Delta=10\omega_z$, $\alpha=2\times10^{-3}$) to the overdamped regime (thin line, $\Delta=3\omega_z$, $\alpha=4\times10^{-3}$), in the high-temperature limit of a spin-boson model with $N=50$ ions, $T=250\omega_z$, $\epsilon=0$. (b) NIBA time kernels corresponding to these two regimes.

LOW-TEMPERATURE REGIME

For the ohmic model in the continuum and scaling limits, the evolution of $P(t)$ at $T=0$ is determined by the value of α, in such a way that there are three regimes to be considered [1]: $\alpha<\frac{1}{2}$ (coherent oscillations), $\frac{1}{2}<\alpha<1$ (overdamped relaxation), and $\alpha>1$, in which case dissipation impedes the decay of $P(t)$ and the system becomes localized in the initial value of the effective spin [17]. This result is related to the quantum Zeno effect, because the spin relaxation is hindered by the measurement performed by the phonons [18]. Since the NIBA is known to reproduce the transition between these three regimes [19], we can use it to investigate whether the mesoscopic ohmic spin-boson model shows the same transition. Figure 4 shows our results, illustrating that the relaxation of $P(t)$ shows the same qualitative features as in the standard ohmic model, but with the additional appearance of quantum revivals at long times. The localization of the spin state is clearly evident at values of $\alpha>1$, although a residual relaxation process still persists as a consequence of the discreteness of the bath. To quantify in more detail the transition to spin localization, we have calculated the initial decay rates at short times, as a function of α. Our results in Fig. 5(a) show the slowing down of the spin relaxation with increasing α, as well as the effect of finite temperatures. Note that Fig. 5(a) corresponds to the finite-size version of the quantum phase transition to localization, which is found in the ther-

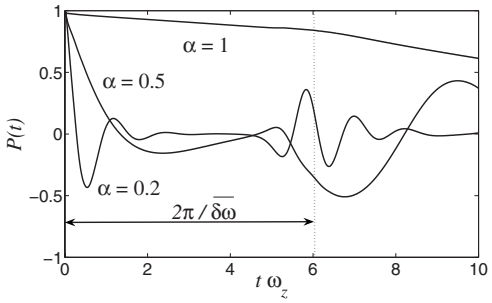

FIG. 4. Spin evolution in the mesoscopic ohmic spin-boson model, in a Coulomb chain with $N=50$ ions, $T=0$, $\Delta=10\omega_z$, $\epsilon=0$, and different dissipation strengths.

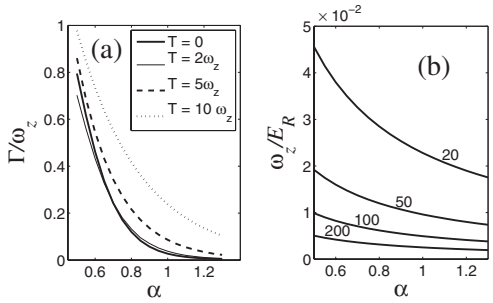

FIG. 5. (a) Evolution of the decay rate in the strong dissipation regime. $N=50$, $\Delta=10\omega_z$. (b) Axial trapping frequency of the trap that is required as a function of dissipation strength in units of the recoil energy, with different values of N. $E_R=k^2/2m$, with k the wave vector in Eq. (3). For example, Be^+, $2\pi/k=313$ nm, yields $E_R=225$ kHz.

modynamic limit of the phonon bath (where Γ would vanish above $\alpha=1$).

The strong dissipation regime of the mesoscopic ohmic spin-boson model requires high values of α, and thus of $(k\bar{z}_1)^2 \propto 1/\omega_z$. In the case of a chain with $N=50$ ions, the transition to localization can be observed with ω_z of a few kHz. The axial trapping frequency that is required to realize a model with a given α decreases with N; see Fig. 5(b). This condition is difficult to meet in an experiment, due to the need to cool the Coulomb chain to low temperatures. However, it must be noted that ground-state cooling is not required. Our calculations show that up to temperatures of the order of the axial trapping frequency, the transition to localization can still be observed, whereas at higher temperatures it is smeared out.

OUTLOOK

Let us comment on the possibility of implementing various interesting experimental situations other than the ones discussed above. In particular, the coupling (2) allows us to implement a bath with $1/f$ noise, a model that is relevant to the description of decoherence of solid-state qubits (both normal and superconducting) [20]. Besides that, according to our discussion for the case of an off-resonant standing wave addressing the central ion, Eq. (2), it is possible to tune the spin-boson coupling in such a way that we implement couplings quadratic in the bath coordinate. Again, these are of current concern in the description of superconducting solid-state qubits operating at the "sweet spot" [21], and could be studied in much more detail in an ion chain model. Finally, the simultaneous coupling of several spins to the vibrational bath, by addressing several ions with lasers, would represent an implementation of a "many spin-boson" model, where the interplay between the phonon bath-mediated spin-spin coupling and dissipation could be studied.

ACKNOWLEDGMENTS

This work was supported by EU projects (SCALA and CONQUEST), the DFG through SFB 631, NIM, and an Emmy-Noether grant (F.M.).

[1] A. J. Leggett *et al.*, Rev. Mod. Phys. **59**, 1 (1987).
[2] U. Weiss, *Quantum Dissipative Systems* (World Scientific, Singapore, 1999).
[3] J. S. Pentillä, U. Parks, P. J. Hakonen, M. A. Paalanen, and E. B. Sonin, Phys. Rev. Lett. **82**, 1004 (1999).
[4] T. Hayashi, T. Fujisawa, H. D. Cheong, Y. H. Jeong, and Y. Hirayama, Phys. Rev. Lett. **91**, 226804 (2003).
[5] D. Porras and J. I. Cirac, Phys. Rev. Lett. **92**, 207901 (2004); **93**, 263602 (2004).
[6] J. P. Barjaktarevic, G. J. Milburn, and R. H. McKenzie, Phys. Rev. A **71**, 012335 (2005).
[7] D. Leibfried *et al.*, Rev. Mod. Phys. **75**, 281 (2003).
[8] D. M. Meekhof, C. Monroe, B. E. King, W. M. Itano, and D. J. Wineland, Phys. Rev. Lett. **76**, 1796 (1996).
[9] G. Morigi and S. Fishman, J. Phys. B **39**, S221 (2006).
[10] D. H. E. Dubin and T. M. O'Neil, Rev. Mod. Phys. **71**, 87 (1999).
[11] W. M. Itano *et al.*, Science **279**, 686 (1998); T. B. Mitchell *et al.*, *ibid.* **282**, 1290 (1998).
[12] D. Porras, J. I. Cirac, S. Kilina, S. Tretiak, and E. Einarsson, Phys. Rev. Lett. **96**, 250501 (2006).
[13] R. Bulla, N.-H. Tong, and M. Vojta, Phys. Rev. Lett. **91**, 170601 (2003).
[14] This problem is related to that of a Kondo impurity in a finite-size metal; see W. B. Thimm, J. Kroha, and J. von Delft, Phys. Rev. Lett. **82**, 2143 (1999).
[15] H. Dekker, Phys. Rev. A **35**, 1436 (1987).
[16] J. Wilkie, Phys. Rev. E **68**, 027701 (2003).
[17] A. J. Bray and M. A. Moore, Phys. Rev. Lett. **49**, 1545 (1982).
[18] A. Peres, Am. J. Phys. **48**, 931 (1980).
[19] R. Egger and C. H. Mak, Phys. Rev. B **50**, 15210 (1994).
[20] Y. Nakamura, Y. A. Pashkin, T. Yamamoto, and J. S. Tsai, Phys. Rev. Lett. **88**, 047901 (2002).
[21] Y. Makhlin and A. Shnirman, Phys. Rev. Lett. **92**, 178301 (2004).